Received 3 January 2007
Revised 11 December 2007
Accepted 19 December 2007

Developing laminar mixed convection of nanofluids in an inclined tube with uniform wall heat flux

R. Ben Mansour and N. Galanis
Faculty of Engineering, Université de Sherbrooke, Sherbrooke, Canada, and
C.T. Nguyen
Faculty of Engineering, Université de Moncton, Moncton, Canada

Abstract

Purpose – The aim is to study the conjugate problem of developing laminar mixed convection flow and heat transfer of water-Al_2O_3 nanofluid inside an inclined tube submitted to a uniform wall heat flux.

Design/methodology/approach – The set of non-linear, coupled and fully elliptic governing equations has been solved using a "finite-control-volume" numerical method, the classical power-law scheme for computing heat and momentum fluxes staggered and non uniform grids for spatial discretization of various regions of the tube.

Findings – Numerical results have shown that the presence of nanoparticles slightly intensifies the secondary flow due to buoyancy, in particular in the developing region. It also increases the average Nusselt number and decreases slightly the product ReC_f with respect to those of water. For the horizontal inclination, two new correlations have been proposed to calculate these two variables in the fully developed region, for Grashof number ranging from 10^3 to 10^5 and particle volume concentrations up to 7 per cent.

Practical implications – The results of this study can be employed for various practical heat transfer and thermal applications using nanofluids.

Originality/value – The present study constitutes an original contribution to the knowledge of nanofluid thermal behaviour.

Keywords Heat transfer, Flow, Convection, Nanotechnology, Numerical analysis

Paper type Research paper

Nomenclature

C_p	specific heat of fluid ($J\,kg^{-1}\,K^{-1}$)	Gr	Grashof number, $Gr = \rho^2 g\beta q_o D^4/\mu^2$
C_f	friction coefficient	h	heat transfer coefficient ($W\,m^{-2}\,K^{-1}$)
D	tube inside diameter (m)		

This project is part of the R&D program of the NSERC Chair in Industrial Energy Efficiency established in 2006 at "*Université de Sherbrooke*". The authors acknowledge the support of the Natural Sciences and Engineering Research Council of Canada, Hydro Québec, Alcan International Ltd and Natural Resources Canada. Thanks are also due to the *Université de Moncton* for financial support to this project as well as to the Faculty of Engineering of the *Université de Sherbrooke* for the scholarship awarded to Mr R. Ben Mansour.

International Journal of Numerical Methods for Heat & Fluid Flow
Vol. 19 No. 2, 2009
pp. 146-164

0961-5539
DOI 10.1108/09615530910930946

k	fluid thermal conductivity ($Wm^{-1}K^{-1}$)
Nu	Nusselt number, $Nu = h\,D/k$
Pr	Prandtl number, $Pr = C_p\mu/k$
q_i	interfacial heat flux (Wm^{-2})
q_o	imposed heat flux (Wm^{-2})
r	radial coordinate (m)
R	normalized radial co-ordinate, $R = r/D$
Re	Reynolds number, $Re = \rho\, u_0 D/\mu$
T	temperature (K)
u_o	average inlet axial velocity ($m\,s^{-1}$)
V_r	normalized radial velocity $= (\rho C_p v_r D/k)$
V_Z	normalized axial velocity $(= v_z/u_0)$
V_ϕ	normalized tangential velocity $(= \rho C_p v_\phi D/k)$
z	axial co-ordinate (m)
Z	normalized axial co-ordinate $(= z/PrReD)$

Greek letters

α	inclination angle over horizontal
Θ	dimensionless temperature, $(= k(T-T_0)/Dq_0)$.
μ	fluid dynamic viscosity ($kg\,m^{-1}\,s^{-1}$)
ρ	fluid density ($kg\,m^{-3}$)
ϕ	angular coordinate
φ	particle volume concentration
Φ	viscous dissipation

Subscripts

0	reference value
b	bulk
bf	base fluid (water)
max	maximum
min	minimum
nf	nanofluid
p	particle
w	wall

1. Introduction

Modern nanotechnology has permitted the fabrication of materials with average size below 50 nm. Fluids formed of saturated liquid and suspended nanoparticles are called nanofluids, a term first used by Choi (1995). Relevant experimental data see in particular, Masuda *et al.* (1993), Choi (1995) and Lee *et al.* (1999), have shown that nanofluids possess superior heat transfer properties compared to those of ordinary fluids. Such studies also indicate that these suspensions are quite stable because of the very small particle size. Thus, nanofluids can constitute a promising alternative for advanced thermal applications, in particular for micro/nano-heat transfer applications where the current tendency towards smaller and lighter heat exchanger systems is considerable (Lee and Choi, 1996; Koo and Kleinstreuer, 2005).

In order to explain the enhancement of nanofluid thermal conductivity, researchers have proposed different mechanisms. Keblinski *et al.* (2002) and Eastman *et al.* (2001) have attributed it to several factors such as the Brownian motion of nanoparticles, the molecular level layering of the liquid at the liquid/particle interface, the phonon heat transport inside nanoparticles and the effects due to particle clustering. On the other hand, Xuan and Li (2000) and Xuan and Roetzel (2000) stipulated that the improvement of effective thermal conductivity of nanofluids is due to the increase of the contact surface between the particles and the fluid as well as to the interaction and collision between them. These authors have also introduced the concept of thermal dispersion due to nanoparticles. It is worth mentioning that Khaled and Vafai (2005) have studied the effect due to thermal dispersion on the heat transfer characteristics of nanofluids.

Their numerical results have shown that the presence of dispersive elements resulted in a 21 per cent augmentation of the Nusselt number for a uniformly heated tube.

However, there are no general models which may satisfactorily explain the strong heat transfer enhancement due to nanofluids as well as to accurately determine their properties. Most of the first experimental and theoretical studies were conducted to determine the nanofluid effective thermal conductivity (Masuda *et al.*, 1993; Choi, 1995; Pak and Cho, 1998; Lee *et al.*, 1999; Wang *et al.*, 1999; Eastman *et al.*, 1999; Xuan and Li, 2000; Eastman *et al.*, 2001). Some studies also provide data for the nanofluid effective viscosity (Masuda *et al.*, 1993; Pak and Cho, 1998; Wang *et al.*, 1999). Wang and Mujumdar (2006) presented a review of recent researches on the heat transfer characteristics of nanofluids.

Several numerical and experimental works have been carried out to study the hydrodynamic and thermal behaviour of nanofluids in confined flows. For forced convective heat transfer, Pak and Cho (1998) studied the heat transfer behaviour in heated tubes and observed that, for a given Reynolds number, the convective heat transfer coefficient increased with increasing volume concentration. They provided the first correlation for computing the Nusselt number for turbulent regime. Li and Xuan (2002) investigated experimentally the convective heat transfer and flow characteristics in a tube with a constant heat flux at the wall. From data collected on nanofluids composed of water and Cu, TiO_2 and Al_2O_3 particles, they proposed empirical correlations for the Nusselt number in both laminar and turbulent flows. Wen and Ding (2004) experimentally studied a water–Al_2O_3 mixture under laminar flow regime in the entrance region of a horizontal heated tube. Yang *et al.* (2005) measured the convective heat transfer coefficient of nanofluids composed of transmission fluids and graphitic-based nanoparticles. Results from the above experimental works have shown that the presence of nanoparticles produces a clear increase of heat transfer. The nanofluids give a higher heat transfer coefficient than the base-fluid for given Reynolds number, and such enhancement becomes more significant with an augmentation of particle concentration. Recent numerical results have also confirmed such beneficial effects for water–γAl_2O_3 and Ethylene Glycol–γAl_2O_3 nanofluids in two confined flows, in particular Maïga *et al.* (2005, 2006) and Roy *et al.* (2004, 2006). It is worth mentioning that similar heat transfer enhancement resulting from the use of nanofluids in a liquid cooling system destined for electronic components has also been investigated (Nguyen *et al.*, 2007; Maré *et al.*, 2006).

For buoyancy-driven flow and heat transfer using nanofluids, very few studies have been carried out. Khanafer *et al.* (2003) were likely the first who studied numerically the natural convection of nanofluid inside a two–dimensional enclosure. Their results show that the heat transfer rate increases with the nanoparticles concentration for a given Grashof number. They observed that the presence of particles can alter the internal flow structure. Ben Mansour *et al.* (2006) studied numerically the conjugate problem of laminar mixed convection flow of Al_2O_3–water nanofluid in a uniformly heated horizontal tube. They found that that the presence of nanoparticles intensifies the buoyancy induced secondary flow, especially in the developing region. Their results also show an augmentation of the heat transfer coefficient and a decrease of the wall friction when using nanofluids. Regarding experimental data, one must cite the pioneering works by Putra *et al.* (2003) who have considered the natural convection of CuO–water and Al_2O_3–water mixtures inside a horizontal cylinder heated at one end and cooled at the other. They observed a clear deterioration of the convective heat transfer coefficient when using nanofluids. Wen and Ding (2005) presented their experimental observations on natural convection of TiO_2–water in a space between

two horizontal aluminium discs. They found that the convective heat transfer coefficient decreases as compared to that of pure water and proposed several mechanisms to explain this deterioration of heat transfer. These experimental data and numerical results clearly show that the heat transfer behaviour of nanofluids is still not very well understood. To our knowledge, there are no other studies considering mixed convection tube flow of nanofluids, especially for inclined tubes.

In the present work, we have investigated numerically the conjugate problem of developing laminar mixed convection flow of a particular nanofluid, Al_2O_3–water mixture, inside an inclined tube submitted to a uniform heat flux on its outside surface.

2. Mathematical description of the problem

2.1 Governing equations and boundary conditions

We consider the problem of fluid flow and heat transfer inside an inclined tube that is submitted to a uniform wall heat flux on a major portion (L2 = 200D) of its length. In order to take into consideration, the effects due to the axial diffusion of heat and momentum, two adiabatic sections are considered upstream and downstream of the heated section, (Figure 1).

The following assumptions have been adopted:

- the flow is steady and laminar;
- the nanofluid under study is considered to behave as a homogenous, incompressible, single-phase Newtonian fluid; and
- all thermal and physical properties of the nanofluid are assumed constant except for the fluid density in the buoyancy force, for which the classical Boussinesq assumption prevails.

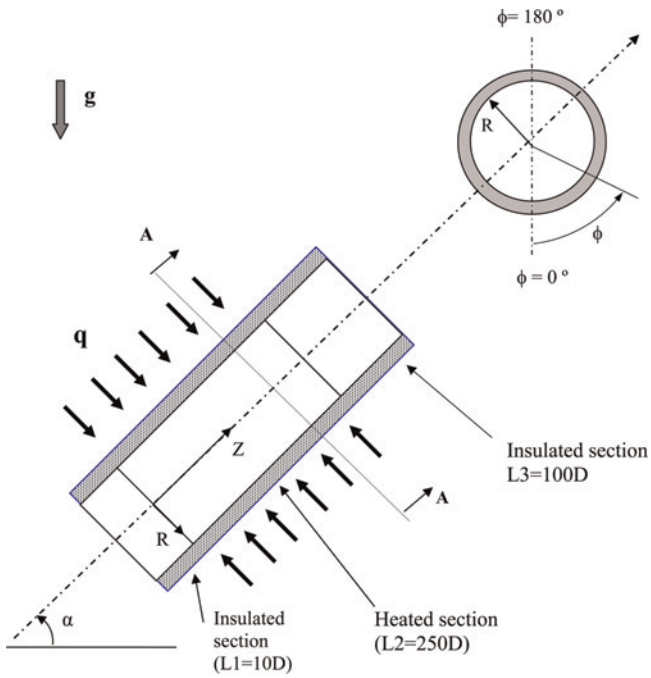

Figure 1.
Schematic representation of the problem under study

2.1.1 Justification of the single-phase Newtonian fluid assumption. Most nanofluids used for heat transfer enhancement are composed of very fine particles, usually < 50 nm. Such reduced dimension of particles may rend them easily fluidized and the resulting liquid–nanoparticle mixture can be considered to behave more like a fluid than a heterogeneous mixture. Furthermore, by assuming that the thermal equilibrium conditions prevail and there is negligible slip between phases, such a mixture can be considered as a homogenous and single-phase fluid. As a consequence of this important assumption, the classical theory developed for single-phase fluids can be directly extended to nanofluids. It is worth noting that, although more experimental data will be needed in order to rigorously assess this assumption, it seems to be validated to some extent through the experimental results by Pak and Cho (1998) and Li and Xuan (2002). These studies have found that nanofluids heat transfer can be appropriately characterised by correlations that are similar to the well-known Dittus–Boelter formula. Further evidence of the validity of this assumption is provided by our recent numerical analyses for nanofluid flow in tubes (Maïga *et al.* 2005, 2006; Ben Mansour *et al.*, 2006; Akbari and Behzadmehr, 2007). On the other hand, the experimental data obtained by Putra *et al.* (2003) for the shear rate-deformation characteristics of a water–Al_2O_3 mixture with particle volume concentrations 4 per cent seems to confirm the Newtonian behaviour of nanofluids. Furthermore, their results indicated that the thermal behaviour of nanofluids is identical to that of a pure fluid. It is worth mentioning that the single-phase fluid model is much simpler and computationally more efficient than a two-phase fluid model (Wang and Mujumdar, 2006).

Under the above assumptions, the general conservation principles are expressed by equations (1) to (3) for the fluid zone and equation (4) for the tube wall:

$$div(\rho \mathbf{V}) = 0 \tag{1}$$

$$div(\rho \mathbf{V} V_i) = -grad\ P + \mu \nabla^2 V_i + \rho_o(1 - \beta(T - T_o))\mathbf{g} \tag{2}$$

$$div(\rho \mathbf{V} C_p T) = div(k\ grad\ T) + \Phi \tag{3}$$

$$div(k_s\ grad\ T) = 0 \tag{4}$$

where the components of the gravitational acceleration vector $\mathbf{g}$ depend on the angular co-ordinate and the tube inclination, and V_i is a velocity component.

As boundary conditions, we have assumed a Poiseuille parabolic axial velocity profile and a uniform fluid temperature at the inlet section, i.e. at $Z = -\mathrm{L1}$. At the outlet section, $Z = \mathrm{L2} + \mathrm{L3}$, outflow condition are applied (i.e. second order axial derivatives are set equal to zero). On the inner surface of the tube wall the usual non-slip condition prevails while the temperature and heat flux in the solid and fluid are identical at this interface. On the outer surface of the tube an axially and circumferentially constant heat flux is imposed for $0 \leq Z \leq \mathrm{L2}$, whereas for $-\mathrm{L1} \leq Z \leq 0$ and $\mathrm{L2} \leq Z \leq \mathrm{L3} + \mathrm{L2}$ this surface is adiabatic.

2.1.2 Determination of Al_2O_3–water nanofluid properties. By assuming uniform particle volume concentration throughout the domain, the nanofluid effective properties can then be computed using classical relations developed for a two-phase mixture (Pak and Cho, 1998; Xuan and Roetzel, 2000). In the following equations, all

fluid properties are evaluated at the reference temperature that is the fluid inlet temperature.

$$\rho_{nf} = (1-\varphi)\rho_{bf} + \varphi\rho_p \tag{5}$$

$$(\rho C_p)_{nf} = (1-\varphi)(\rho C_p)_{bf} + \varphi(\rho C_p)_p \tag{6}$$

$$(\rho\beta)_{nf} = (1-\varphi)(\rho\beta)_{bf} + \varphi(\rho\beta)_p \tag{7}$$

$$\mu_{nf} = \mu_{bf}(123\varphi^2 + 7.3\varphi + 1) \tag{8}$$

$$\frac{k_{nf}}{k_{bf}} = \frac{k_p + 2k_{bf} - 2\varphi(k_{bf} - k_p)}{k_p + 2k_{bf} + \varphi(k_{bf} - k_p)} \tag{9}$$

In order to compute the dynamic viscosity of the nanofluid under consideration, equation (8) has been obtained by performing the least-square curve fitting of experimental data by Wang *et al.* (1999). Regarding the nanofluid thermal conductivity, although some experimental data do exist, they remain rather scarce and exhibit a large dispersion. Therefore, we have adopted the well-known Hamilton and Crosser (1962) model, equation (9), assuming spherical nanoparticles. More details and discussion regarding the determination of nanofluid properties have been presented elsewhere (Maïga *et al.*, 2005).

2.2 Numerical method and code validation

The non-linear, coupled and fully elliptic governing equations (1) to (4) have successfully been solved using a numerical method based on the finite-control-volume approach (Patankar, 1980; Fluent, 2005). The classical power-law scheme has been adopted to compute the combined convection-and-diffusion fluxes of heat and momentum. An extensive study of grid influence was carried out and the non-uniform and staggered grid $34(r) \times 40(\phi) \times 700(z)$ has been adopted. The nodes are highly packed in the vicinity of the solid-fluid interface, the inlet section and in the areas close to the interfaces between the heated and adiabatic sections. The grid spatial increment remains uniform in the circumferential direction. The convergence criteria are based on the residues resulting from the spatial integration of the governing equations on finite volumes. For cases performed in this study, residues were always kept lower than at least 10^{-6}, for all the equations of conservation.

The numerical code, implemented on a parallel-processors computer, has been extensively validated by comparing the numerical results obtained for various cases of forced and mixed convection flows and heat transfer to analytical results as well as to experimental data available in the literature. In particular, several validation tests have also been performed for the case of mixed laminar convection flow of water in horizontal tube with uniform wall heat flux. Details and results regarding the code validation have been presented in another recent paper (Ben Mansour *et al.* 2006).

3. Results and discussion

The problem studied can be characterized by four dimensionless parameters, namely the particle volume concentration φ, the Grashof number Gr, the flow Reynolds number Re and the tube inclination α. In this paper, extensive numerical simulations have been carried out for a copper tube, various tube inclination and several values of the Grashof number. The results and discussion presented here focus on the effects of particle volume concentration on the flow and heat transfer behavior of the nanofluid.

3.1 Development of the flow and thermal fields for a tube inclination $\alpha = 30°$

In the following section, we present some typical results, illustrated in Figures 2 to 8, for Al_2O_3–water nanofluid, four different particle concentrations, $\varphi = 0$, 3, 5 and 7 per cent, $Re = 100$, $Gr = 10^4$ and $\alpha = 30°$. For a good comprehension of these results, it should be noted that the upstream adiabatic section corresponds to $Z < 0$, the heated section extends from $Z = 0$ to $Z \approx 0.3$ and the downstream adiabatic section corresponds to $Z > 0.3$.

3.1.1 Heat flux at solid/liquid interface. Figure 2 shows the circumferential variation of the ratio q_i/q_0 for four particular axial locations, namely $Z = -0.00574$, 0.0286, 0.0714 and 0.393 (or, equivalently, $z = -8D$, $z = 20D$, $z = 50D$ and $z = 275D$). Because of the heat conduction in the tube wall, the heat flux distribution at the wall-liquid interface is not uniform circumferentially. Furthermore, the ratio q_i/q_0 is axially dependent. In the upstream adiabatic zone, the interface heat flux increases with an increase of Z but remains circumferentially uniform. In the heated section i.e. for $0 \leq Z \leq 0.3$, heat transferred from the tube wall to the fluid increases considerably, in particular in the lower region due to heat conduction in the tube wall. In the downstream adiabatic section, the interfacial heat flux decreases with the axial coordinate. The ratio q_i/q_0 even reaches negative values in the upper part of the tube, which indicates that heat is transferred from the hot fluid towards the tube wall. This heat is then conducted circumferentially through the wall and transferred to the cold fluid near the bottom of the tube. Thus, the fluid temperature becomes more uniform. It is important to note that the effect of particle concentration on the interfacial heat flux appears insignificant because the thermal conductivity of the nanofluid is too low with respect to that of the copper wall. These results are qualitatively similar to those obtained numerically by Ben Mansour *et al.* (2006) for mixed convection in a horizontal tube.

3.1.2 Structure of the flow and thermal fields. Figure 3 shows the secondary flow structure at two axial positions in the heated section ($Z = 0.00714$ and 0.0714) for $\varphi = 0$ and 7 per cent. Near the inlet of the heated section (not shown), i.e. in the absence of free convection, the tangential components of velocities are zero and velocity vectors are radial and directed towards the tube center. At $Z = 0.00714$, one can notice the formation of the buoyancy-driven flow. Such flow is characterised by an ascendant

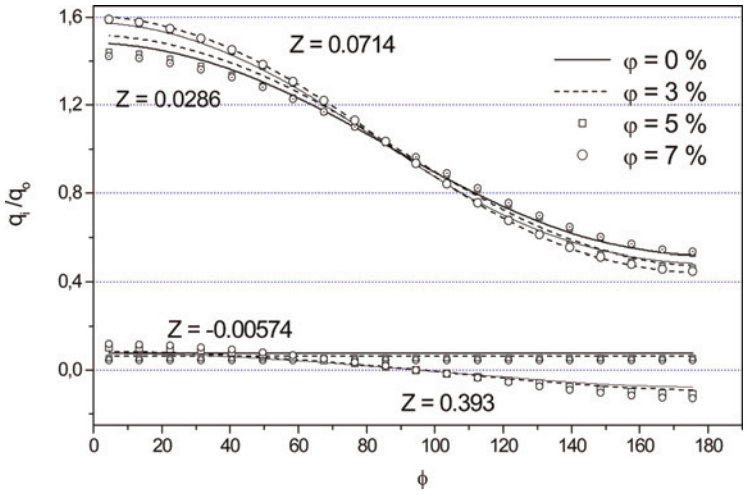

Figure 2.
Circumferential variation of the interfacial heat flux for $\alpha = 30°$, $Re = 100$ and $Gr = 10^4$

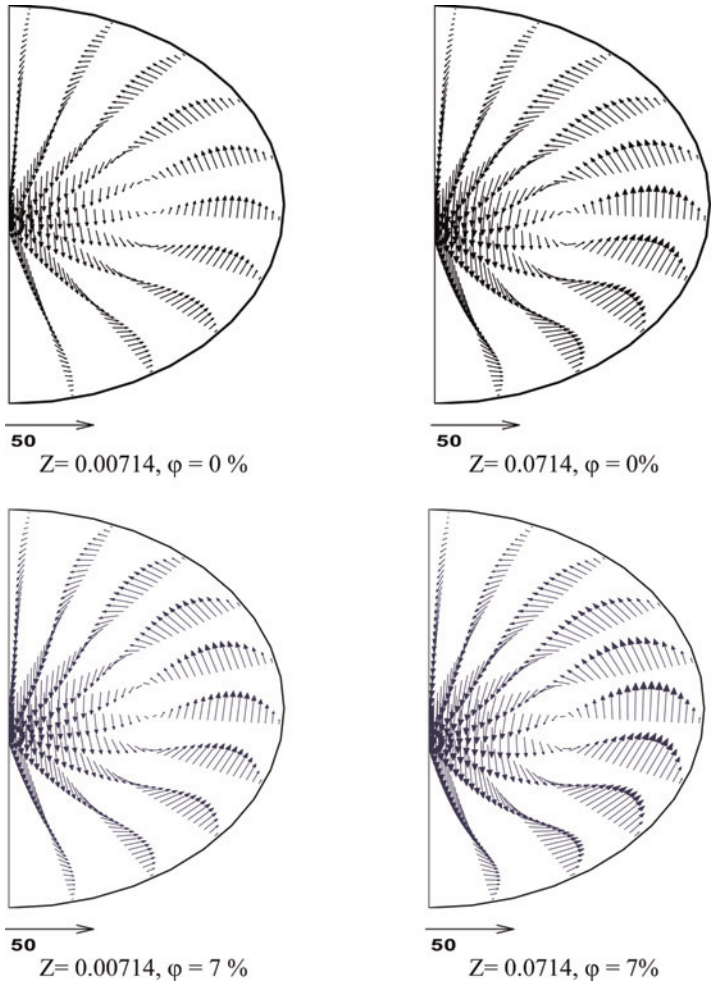

Figure 3.
Development of secondary flow field for $\varphi = 0$ and $\varphi = 7$ per cent ($\alpha = 30°$, $Re = 100$ and $Gr = 10^4$)

movement of fluid along the tube wall and a downward movement along the main diameter in the central region. Within a short distance from the entrance of the heated section, the buoyancy-induced flow is mainly confined in the vicinity of the tube wall. Farther downstream, this secondary flow increases progressively in intensity with a presence of an intense recirculation zone. At $Z = 0.0429$ in particular (not shown), the magnitude of the secondary velocities are maximal. With further increase of axial co-ordinate in the heated section, at $Z = 0.0714$, under a strong stratification due to heating effect, the secondary flow decreases slightly in intensity to reach a certain asymptotic state. It is also interesting to note that an increase of particle volume concentration is only manifested by a slight intensification of the secondary currents. The latter seem to develop more rapidly with respect to the base fluid. This behaviour is explained by the fact that for a given Grashof number, an increase of particle volume concentration necessitates a higher imposed heat flux q_0 and therefore, results in a more pronounced secondary flow.

Figure 4 shows the isotherms at four axial positions in the heated section for $\varphi = 0$ and 7 per cent. Note that for the sake of clarity, values of the dimensionless temperature were given only for three or five different temperature levels. We observe that near the entrance of the heated section, $Z = 0.00714$ in particular, where the inner surface of the tube is circumferentially close to isothermal, all isotherms in the fluid are circular and concentric and unaffected by the secondary flow which is still weak. At this section, the effect of particle volume concentration is negligible. As the fluid moves farther downstream, the buoyancy effect becomes stronger and affects the temperature field. The isotherms become distorted, especially in the central and the upper parts of the section. At $Z = 0.0286$ for example, the temperature field exhibits drastic distortions with nearly horizontal isotherms in the central/upper region while colder fluid is confined inside a narrow lower part of the section. The presence of nanoparticles modifies slightly the structure of the thermal field. Thus, for a given axial location, the isotherms for $\varphi = 7$ per cent have become much more distorted. The temperature

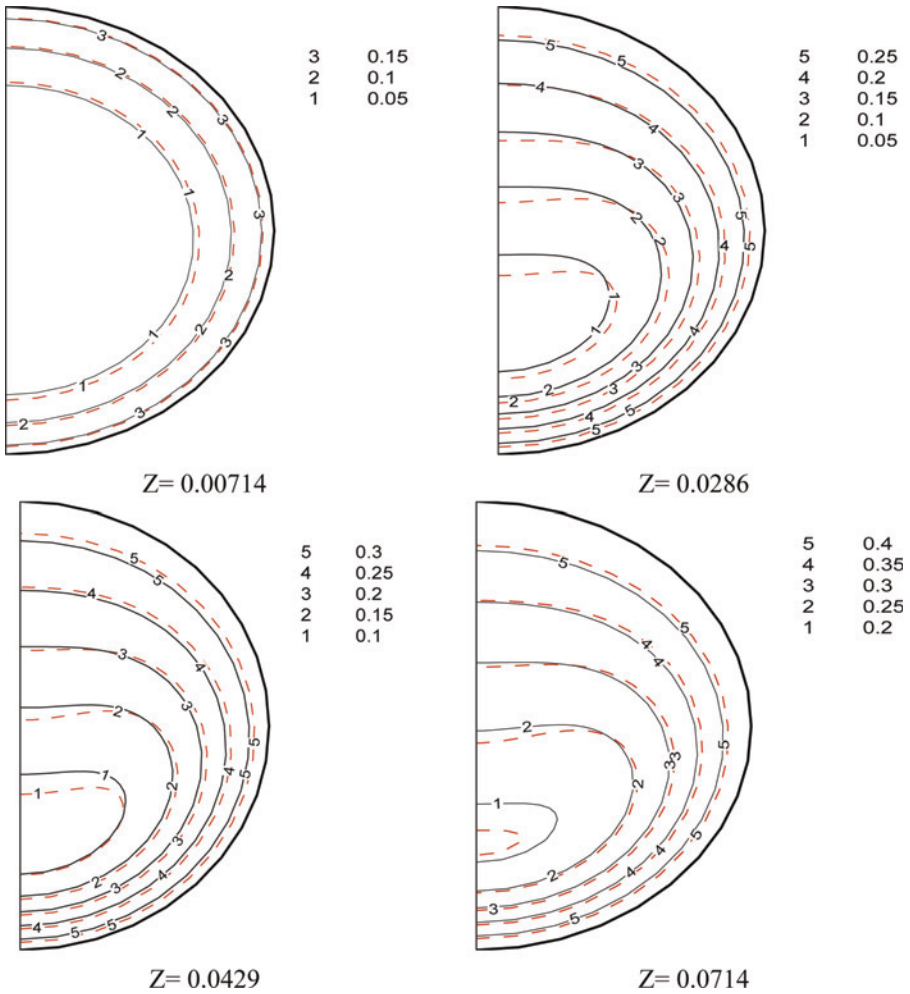

Figure 4.
Development of temperature field ($\varphi = 0$: ———— and $\varphi = 7$ per cent: ------) for $\alpha = 30°$, $Re = 100$ and $Gr = 10^4$ (numbers associated with lines 1 to 5 indicate the value of the dimensionless temperature)

gradient is more important, indicating a stronger buoyancy effect with higher particle concentration. With an increase of φ, the temperature stratification inside the fluid also becomes more pronounced and affects a larger area of the section, especially in the upper and central parts. Furthermore, the cold fluid zone in the lower part and the position of the minimum fluid temperature move slightly downwards as φ increases. It is very interesting to mention that these results are qualitatively consistent with the experimental data by Nnanna *et al.* (2004) and the numerical results by Khanafer *et al.* (2003) for natural convection of nanofluids inside a two-dimensional-enclosure.

3.1.3 Temperature profiles. Figure 5 shows the dimensionless temperature profiles along the vertical diameter ($\phi = 0$, $\phi = \pi$) for four axial positions and four different particle concentrations. At the entrance of the heated section, $Z = 0$, the wall heating effect on the fluid temperature is manifested inside a thin layer near the tube wall and is essentially symmetrical with respect to the tube axis. Further downstream, distortions of the temperature profile become visible, especially in the lower part near the tube wall. In the upper region however, the radial variation of fluid temperature is almost linear because of the thermal stratification (cf. Figure 4). In the central lower region where colder fluid is confined, the fluid temperature exhibits a minimum value near the wall. It is interesting to note that the temperature difference in the fluid, expressed by $\Theta_{max} - \Theta_{min}$, decreases with an increase of particle volume concentration. This is due to a stronger buoyancy effect for high particle concentration, which tends to render uniform the fluid temperature. Thus, at $Z = 0.0714$ in particular, the difference $\Theta_{max} - \Theta_{min}$ decreases from 0.263 for $\varphi = 0$ per cent to 0.225 for $\varphi = 7$ per cent.

Figure 6 shows the axial development of the circumferentially averaged interfacial wall temperature Θ_w and the fluid bulk temperature Θ_b for various particle volume concentrations. It is very interesting to observe that due to axial heat conduction in the tube wall, the imposed heating affects both adiabatic zones. In the upstream zone, values of Θ_w are superior to 0. The wall temperatures increase steeply up to the location $Z \approx 0.015$ because of the development of the thermal field. Beyond this position, the fully developed conditions are reached and all temperatures increase linearly with the axial co-ordinate. At a short distance from the end of the heated section (not shown), both Θ_w and Θ_b tend to the same value that is dependent on the overall heat balance. Results in Figure 6 also show that the difference between the fluid

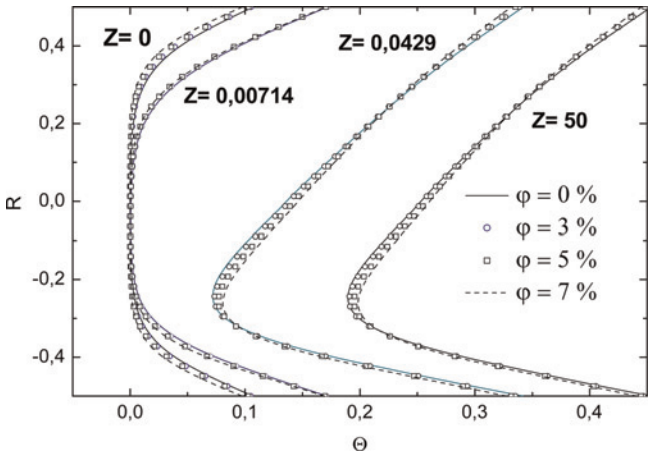

Figure 5.
Temperature profiles along vertical diameter for $\alpha = 30°$, $Re = 100$ and $Gr = 10^4$

temperature and the wall temperature, $\Theta_w - \Theta_b$, decreases slightly with an increase of φ. Thus, in the fully developed flow zone, $Z \geq 0.0429$, $\Theta_w - \Theta_b$ has decreased by nearly 0.008 between cases $\varphi = 0$ and 7 per cent. Such a temperature decrease exists all along the heated section and is more important towards its end.

3.1.4 Axial variation of the Nusselt number and the friction coefficient. Figures 7 and 8 illustrate the axial development of the average Nusselt number and wall friction coefficient, respectively. It is observed that as the axial co-ordinate increases from the inlet of the heated section, the Nusselt number decreases rapidly, reaches a minimum value approximately at the location $Z = 0.0357$ and increases slightly to reach an asymptotic value farther downstream. With regard to the particle volume concentration effect on the Nusselt number, it is observed that near the entrance of the heated section where the free convection effect is still negligible, the curves for all values of φ follow the one corresponding to pure forced convection. As the axial co-ordinate increases, the buoyancy effect becomes more intense (Figures 3 and 4), the temperature difference $\Theta_w - \Theta_b$ becomes constant (Figure 6) and Nu reaches a constant value. Since the

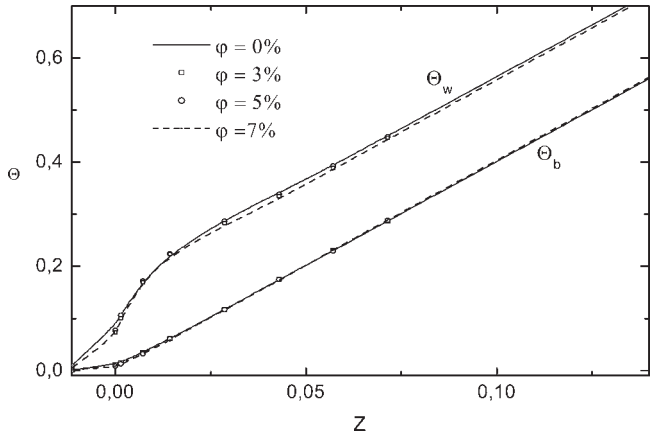

Figure 6.
Axial development of temperature for $\alpha = 30°$, $Re = 100$ and $Gr = 10^4$

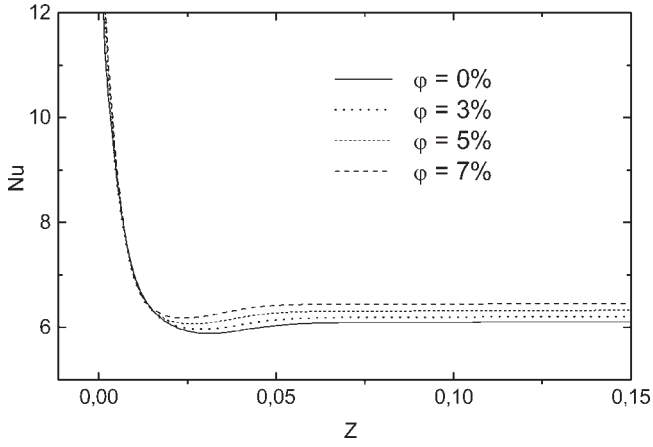

Figure 7.
Axial variation of Nusselt number for $\alpha = 30°$, $Re = 100$ and $Gr = 10^4$

increase of φ reduces the temperature difference $\Theta_w - \Theta_b$, the increase of particle concentration causes an increase of the asymptotic Nusselt number. Thus, for φ increasing from 0 to 7 per cent, an approximate increase of 6 per cent of the asymptotic Nusselt number has been achieved. It is worth noting that the Nusselt values for all particle concentrations are higher than the value 4.364 for pure forced convection.

The influence of nanoparticles on the wall friction coefficient is shown in Figure 8. It is observed that the friction coefficient increases very steeply within a short distance from the inlet of the heated section, and it exhibits a maximum value at $Z \approx 0.0357$, position where the secondary flow effect is most intense. From this position onwards, $C_f Re$ decreases to reach finally an asymptotic value. For the Grashof number considered, $Gr = 10^4$, the effect of nanoparticles on the asymptotic value of $C_f Re$ remains insignificant as the difference with respect to that of water is <1.5 per cent.

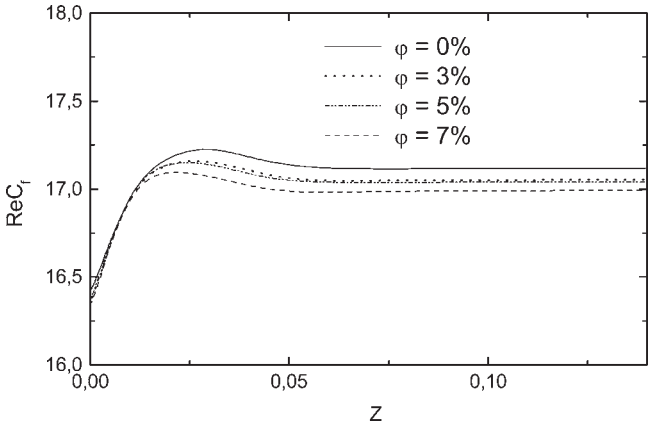

Figure 8.
Axial variation of average wall friction coefficient for $\alpha = 30°$, $Re = 100$ and $Gr = 10^4$

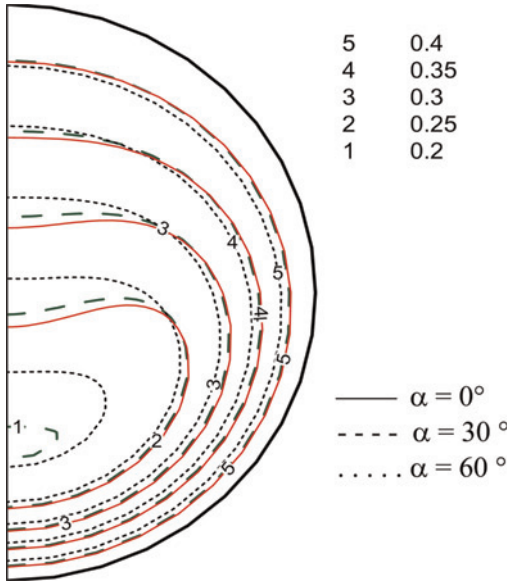

Figure 9.
Effect of the inclination angle on isotherm contours for $\varphi = 7$ per cent at $Z = 0.0429$ (numbers associated with lines 1 to 5 indicate the value of the dimensionless temperature)

3.2 Influence of the tube inclination

Figure 9 shows the effect of inclination on the temperature field for a particle volume concentration of 7 per cent at $Z = 0.0429$. One can observe that as the inclination decreases, the isotherms become more distorted with the strongest buoyancy effect occurring for a horizontal tube configuration. For the latter case, the temperature stratification becomes more important in the central and upper parts of the section, where the isotherms have a tendency to become horizontal. On the other hand, the distortion of the isotherms is small in the bottom part and near the tube wall. It is also noticed that the temperature field tends to become axis-symmetrical when the inclination increases. These results are similar to those obtained numerically by several authors (Cheng and Hong, 1972; Orfi and Galanis, 1993) for the mixed convection of water.

Figure 10 shows the axial variation of the Nusselt number for four inclinations. It is observed that the effect of natural convection is important in a horizontal tube and decreases rapidly as α increases. Therefore, this effect tends to reduce the temperature difference $\Theta_w - \Theta_b$. Then, the Nusselt number is significantly higher for a horizontal case: in the fully developed region, the Nusselt number decreases by nearly 30 per cent when the inclination increases from 0° to 90°. The results for $\varphi = 0$ are in good argument with those calculated by Orfi and Galanis (1993). These results also confirm that the effect of particle concentration observed earlier (Figure 7) prevails for all tube inclinations, with the exception of the vertical tube. In this case, the asymptotic value of *Nu* is independent of φ.

Figure 11 illustrates the influence of the inclination and the particle volume concentration on the average friction coefficient. In a vertical tube, the axial component of the buoyancy force is the highest and this leads to a higher average wall friction coefficient compared to the other case. Thus, the increase of ReC_f in the fully developed region is 16.5 per cent when the inclination angle increases from 0 to 90°. Again, these results confirm that the effect of φ observed earlier (Figure 8) prevails for all tube inclinations, with the exception of the vertical one, where the fully-developed wall friction coefficient is independent of the nanoparticle volume concentration.

3.3 Effect of the Gr number

The effect of the Grashof number and the particle volume concentration on the Nusselt number for a horizontal tube with $Re = 100$ is presented in Figure 12. One can observe

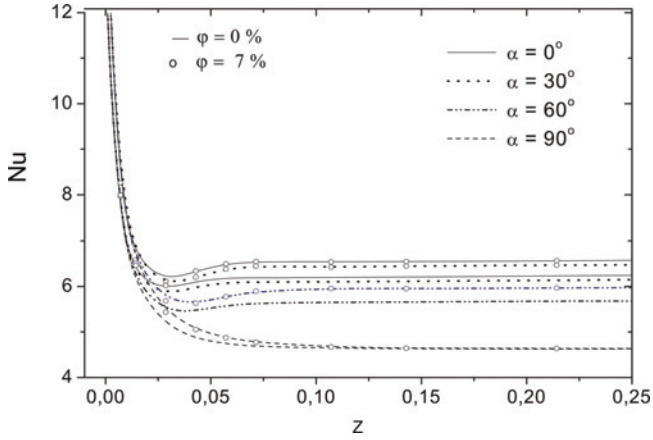

Figure 10.
Effect of the inclination angle on Nusselt number ($\varphi = 0$ per cent and 7 per cent)

that the Nusselt number increases considerably with an augmentation of *Gr*. For example, for $\varphi = 7$ per cent, the Nusselt number increases by about 7 per cent between $Gr = 10^4$ and $Gr = 10^5$. For a given Grashof number, the presence of nanoparticles enhances but only slightly the heat transfer. For example, for $Gr = 10^4$, Nu increases by 5.5 per cent between $\varphi = 0$ and $\varphi = 7$ per cent.

Using the results obtained from the present simulations, the following correlation was determined for the Nusselt number in a horizontal tube as a function of the particle volume concentration ($0 \leq \varphi \leq 7$ per cent), and the Grashof number ($0 \leq Gr \leq 10^5$):

$$Nu = Nu_0(1 + 8\varphi^{1.9}) \cdot \left(1 + \frac{Gr^{1.435}}{35530}\right)^{0.125} \tag{10}$$

Table I shows a comparison of the Nusselt number values as computed by equation (10) and those from the numerical data. The correlation coefficient and the average

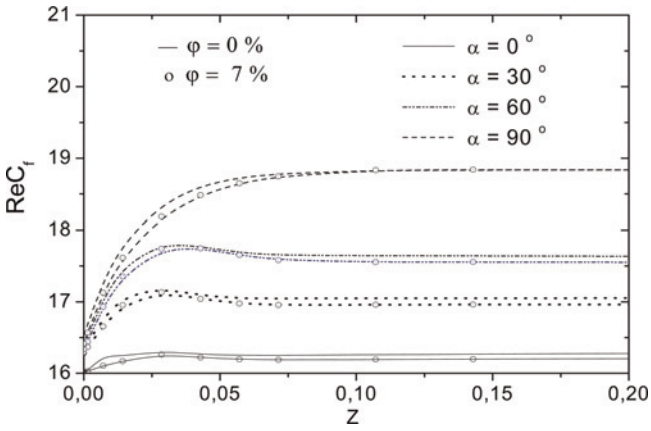

Figure 11.
Effect of the inclination angles on average wall friction coefficient ($\varphi = 0$ per cent and 7 per cent)

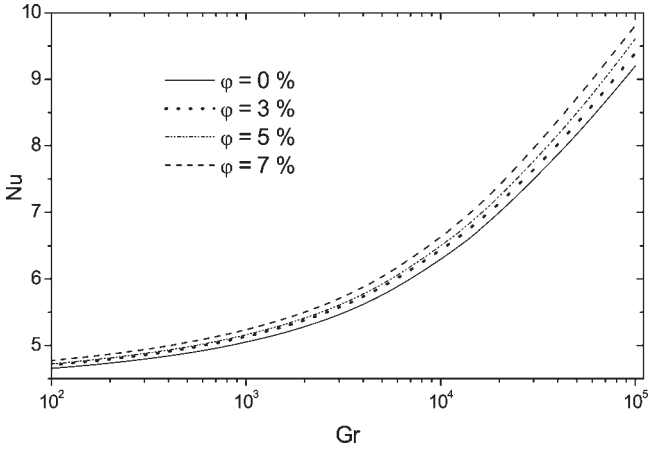

Figure 12.
Effect of Grashof number on the fully developed Nusselt number ($Re = 100$, $\alpha = 0°$)

error are 99.93 per cent and 0.95 per cent respectively. These values show that the proposed correlation is satisfactory within the previously defined ranges of the independent parameters. Furthermore, Figure 13 shows that the proposed correlation is in a very good agreement with experimental (Petukhov and Polyakov, 1967; Morcos, 1974) and numerical (Orfi, 1995) results for water flow in a horizontal tube.

The effect of the volume concentration on the wall friction coefficient is shown in Figure 14 where ReC_f is plotted against the Grashof number. The figure shows that the product ReC_f increases with increasing Grashof number. On the other hand, it decreases slightly with increasing particle volume concentration. Thus, for a given

Grashof number Gr	Particle volume concentration φ (%)	Numerical solution		Relative error (%)
		Numerical solution	Equation (10)	
1,000	0	4.552	4.616	1.44
	3	4.615	4.663	1.19
	5	4.635	4.741	2.42
	7	4.698	4.852	3.49
10,000	0	6.231	6.193	0.57
	3	6.384	6.257	1.96
	5	6.433	6.360	1.10
	7	6.562	6.510	0.76
20,000	0	6.974	6.979	0.16
	3	7.103	7.051	0.71
	5	7.212	7.168	0.56
	7	7.370	7.336	0.43
50,000	0	8.171	8.208	0.88
	3	8.305	8.292	0.06
	5	8.451	8.430	0.21
	7	8.690	8.628	0.68
100,000	0	9.201	9.290	1.01
	3	9.412	9.385	0.13
	5	9.611	9.541	0.69
	7	9.810	9.765	0.42

Table I.
Comparison of numerical results and the Nusselt number correlation (equation(10)) for $Re = 100$

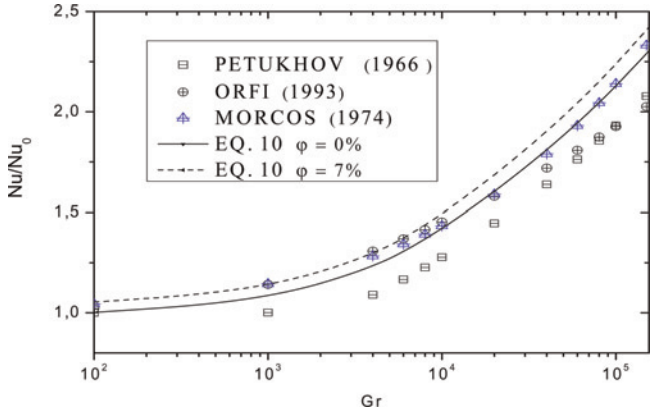

Figure 13.
Comparison of proposed correlation with experimental results and other published correlations ($Re = 100$, $\alpha = 0°$)

Grashof number, the product ReC_f is higher for pure water than for any particle volume concentration. The following new correlation expresses the wall friction coefficient as a function of the particle volume concentration ($0 \leq \varphi \leq 7$ per cent), and the Grashof number ($0 \leq Gr \leq 10^5$):

$$ReC_f = ReC_{f0}\left(1 - 1.32\varphi^{1.78}\right)\left(1 + \frac{Gr^{1.142}}{260200}\right)^{0.125} \quad (11)$$

Table II shows a comparison of the wall friction coefficient values as computed by equation (11) and those from the numerical data. The correlation coefficient and the

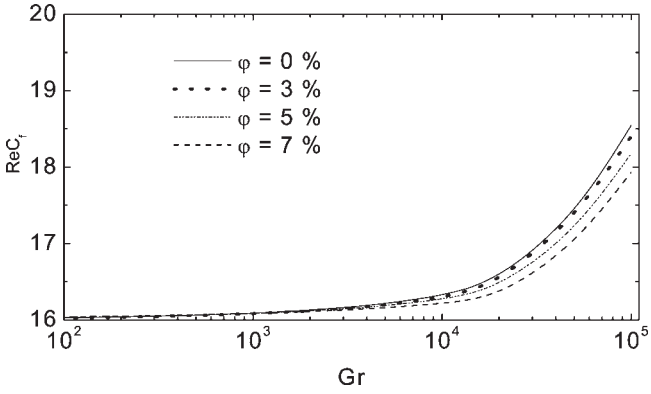

Figure 14.
Effect of Grashof number on average wall friction coefficient in the fully developed region ($Re = 100$, $\alpha = 0°$)

Grashof number Gr	Particle volume concentration φ (%)	Numerical solution	Eequation (11)	Relative error (%)
		Numerical solution		
1,000	0	16.020	16.020	0.003
	3	16.020	15.979	0.254
	5	16.030	15.918	0.697
	7	16.044	15.834	1.306
10,000	0	16.280	16.268	0.074
	3	16.254	16.226	0.171
	5	16.242	16.164	0.479
	7	16.204	16.079	0.771
20,000	0	16.530	16.555	0.152
	3	16.484	16.513	0.173
	5	16.420	16.449	0.179
	7	16.300	16.363	0.386
50,000	0	17.345	17.329	0.094
	3	17.317	17.284	0.189
	5	17.137	17.218	0.474
	7	16.970	17.128	0.929
100,000	0	18.544	18.333	1.138
	3	18.400	18.286	0.620
	5	18.178	18.216	0.209
	7	17.930	18.120	1.060

Table II.
Comparison of numerical results and the wall friction coefficient correlation (equation(11)) for $Re = 100$

average error are 99.26 per cent and 0.47 per cent, respectively. These values show that the proposed correlation is satisfactory within the previously defined ranges of the independent parameters.

4. Conclusion

In this study, we have investigated numerically the conjugate problem of hydrodynamically and thermally developing laminar mixed convection flow of water and water–γAl_2O_3 mixture inside an inclined tube with a uniform wall heat flux on the outside surface. The results have clearly shown that the presence of nanoparticles produces changes on both velocity and temperature fields. These changes are manifested through a rapid development of a slightly more intense secondary flow and a diminution of the fluid bulk temperature. It has been found that a higher particle volume concentration induces an increase of the Nusselt number and a decrease of the product ReC_f for all inclination except the vertical one. Two new correlations have been proposed for computing the average Nusselt number and the product ReC_f for a horizontal tube.

References

Akbari, M. and Behzadmehr, A. (2007), "Developing mixed convection of a nanofluid in a horizontal tube with uniform heat", *International Journal of Numerical Methods for Heat and Fluid Flow*, Vol. 17 No. 6, pp. 566-86.

Ben Mansour, R., Galanis, N. and Nguyen, C.T. (2006), "Developing laminar mixed convection of nanofluids in a horizontal tube with uniform wall heat flux", *Proceedings of the 13th IHTC, Sydney NSW*, pp. 13-18.

Cheng, K.C. and Hong, S.W. (1972), "Combined free and forced laminar convection in inclined tubes", *Appl. Sci. Res*, Vol. 27, pp. 19-38.

Choi, S.U.-S. (1995), "Enhancing thermal conductivity of fluids with nanoparticles", *ASME Publications* FED- 231/MD-66, pp. 99-105.

Eastman, J.A., Choi, S.U.-S., Li, S., Yu, W. and Thompson, L.J. (2001), "Anomalously increase effective thermal conductivities of ethylene glycol-based nanofluids containing copper nanoparticles", *Appl. Phys. Lett*., Vol. 78 No. 6, pp. 718-20.

Eastman, J.A., Choi, S.U.-S., Li, S., Soyez, G., Thompson, L.J. and DiMelfi, R.J. (1999), "Novel thermal properties of nanostructured materials", *Journal of Metastable Nanocrystalline Materials*, Vol. 2-6, pp. 629-34.

Fluent (2005), *Fluent 6 User's Guide*, Fluent Inc., Lebanon, NH.

Hamilton, R.L. and Crosser, O.K. (1962), "Thermal conductivity of heterogeneous two-component systems", *I & EC Fundamentals*, Vol. 1 No. 3, pp. 187-91.

Keblinski, P., Phillpot, S.R., Choi, S.U.-S. and Eastman, J.A. (2002), "Mechanisms of heat flow in suspensions of nano-sized particles (nanofluids)", *International Journal of Heat Mass Transfer*, Vol. 45, pp. 855-63.

Khaled, A.-R.A. and Vafai, K. (2005), "Heat transfer enhancement trough control of thermal dispersion effects", *International Journal of Heat and Mass Transfer*, Vol. 48 No. 11, pp. 2172-82.

Khanafer, K., Vafai, K. and Lightstone, M. (2003), "Buoyancy-driven heat transfer enhancement in a two-dimensional enclosure utilizing nanofluids", *International Journal of Heat Mass Transfer*, Vol. 46, pp. 3639-53.

Koo, J. and Kleinstreuer, C. (2005), "Laminar nanofluid flow in microheat-sinks", *International Journal of Heat Mass Transfer*, Vol. 48, pp. 2652-61.

Lee, S. and Choi, S.U.-S. (1996), "Application of metallic nanoparticle suspensions in advanced cooling systems", *ASME Publications* PVP-Vol. 342/MD-Vol. 72, pp. 227-34.

Lee, S., Choi, S.U.-S., Li, S. and Eastman, J.A. (1999), "Measuring thermal conductivity of fluids containing oxide nanoparticles", *Journal of Heat Transfer*, Vol. 121, pp. 280-9.

Li, Q. and Xuan, Y. (2002), "Convective heat transfer performances of fluids with nano-particles", *Proc. 12th Int. Heat Transfer Conference*, *Grenoble*, p. 483.

Maïga, S.E.B., Palm, S.J., Nguyen, C.T., Roy, G. and Galanis, N. (2005), "Heat transfer enhancement by using nanofluids in forced convection flows", *International Jorunal of Heat Fluid Flow*, Vol. 26, pp. 530-46.

Maïga, S.E.B., Nguyen, C.T., Galanis, N., Roy, G., Maré, T. and Coqueux, M. (2006), "Heat transfer enhancement in turbulent tube flow using Al_2O_3 nanoparticle suspension", *Int. J. Num. Meth. Heat Fluid Flow*, Vol. 16 No.3, pp.275-92.

Maré, T., Schmitt, A.-G., Nguyen, C.T., Miriel, J. and Roy, G. (2006), "Experimental heat transfer and viscosity study of nanofluids: water–γAl_2O_3", *Proceedings of 2nd International Conference Thermal Engineering Theory and Applications, paper no. 93, 3-6 January, Al Ain (to be published)*.

Masuda, H., Ebata, A., Teramae, K. and Hishinuma, N. (1993), "Alteration of thermal conductivity and viscosity of liquid by dispersing ultra-fine particles (dispersion of γ-Al_2O_3, SiO_2 and TiO_2 ultra-fine particles)", *Netsu Bussei* (in Japanese), Vol. 4 No. 4, pp. 227-33.

Morcos, S.M. (1974), "Combined forced and free laminar convection in horizontal tubes", PhD thesis, Iowa State University, Ames, IA, p. 152.

Nguyen, C.T., Roy, G., Gauthier, C. and Galanis, N. (2007), "Heat transfer enhancement using Al_2O_3 water nanofluid for an electronic liquid cooling system", *Applied Thermal Engineering*, Vol. 27 Nos. 8-9, pp. 1501-6.

Nnanna, A.G.A., Fistrovich, T., Malinski, K. and Choi, S.U.-S. (2004), "Thermal transport phenomena in buoyancy-driven nanofluids", *ASME, Electronic and Photonic Packaging*, Vol. 4, pp. 571-8.

Orfi, J. (1995), "Convection mixte laminaire dans un tuyau incliné: développement simultané et phénomène de bifurcation", PhD thesis, Université de Sherbrooke.

Orfi, J. and Galanis, N. (1993), "Laminar fully developed incompressible flow with mixed convection in inclined tubes", *Int. J. Num. Meth. Heat Fluid Flow*, Vol. 3 No. 4, pp. 341-55.

Pak, B.C. and Cho, Y.I. (1998), "Hydrodynamic and heat transfer study of dispersed fluids with submicron metallic oxide particles", *Experimental Heat Transfer*, Vol. 11 No. 2, pp. 151-70.

Patankar, S.V. (1980), *Numerical Heat Transfer and Fluid Flow*, McGraw-Hill, New York, NY.

Petukhov, B.S. and Polyakov, A.F. (1967), "Effect of free convection on heat transfer during forced flow in a horizontal pipe", *High Temperature Research Institute*, Vol. 5, pp. 348-51.

Putra, N., Roetzel, W. and Das, S.K. (2003), "Natural convection of nano-fluids", *Heat and Mass Transfer*, Vol. 39, pp.775-84.

Roy, G., Nguyen, C.T. and Comeau, M. (2006), "Numerical investigation of electronic component cooling enhancement using nanofluids in a radial flow cooling system", *Journal of Enhanced Heat Transfer*, Vol. 13 No. 2, pp. 101-15.

Roy, G., Nguyen, C.T. and Lajoie, P.-R. (2004), "Numerical investigation of laminar flow and heat transfer in a radial flow cooling system with the use of nanofluids", *Superlattices and Microstructures*, Vol. 35 Nos. 3-6, pp. 497-511.

Wang, Q.-X. and Mujumdar, A.S. (2006), "Heat transfer characteristics of nanofluids: a review", *International Journal of Thermal Sciences*, Vol. 46 No. 1, pp. 1-19.

Wang, X., Xu, X. and Choi, S.U.-S. (1999), "Thermal conductivity of nanoparticles-fluid mixture", *Journal of Thermophysics and Heat Transfer*, Vol. 13 No. 4, pp. 474-80.

Wen, D. and Ding, Y. (2004), "Experimental investigation into convective heat transfer of nanofluids at the entrance region under laminar flow conditions", *Internationl Journal of Heat Mass Transfer*, Vol. 47, pp. 5181-88.

Wen, D. and Ding, Y. (2005), "Formulation of nanofluids for natural convective heat transfer applications", *Journal of Heat and Fluid Flow*, Vol. 26 No. 6, pp. 855-64.

Xuan, Y. and Li, Q. (2000), "Heat transfer enhancement of nanofluids*", International. Journal of Heat Fluid Flow*, Vol. 21, pp. 58-64.

Xuan, Y. and Roetzel, W. (2000), "Conceptions for heat transfer correlation of nanofluids", *International Journal of Heat Mass Transfer*, Vol. 43, pp. 3701-7.

Yang Y, Zhang, Z.G., Grulke, E.A., Anderson, W.B. and Wu, G. (2005), "Heat transfer properties of nanoparticle-in-fluid dispersions (nanofluids) in laminar flow", *International Journal of Heat Mass Transfer*, Vol. 48 No. 6, pp. 1107-16.

Further reading

Das, S.K., Putra, N., Thiesen, P. and Roetzel, W. (2003), "Temperature dependence of thermal conductivity enhancement for nanofluids", *Journal of Heat Transfer*, Vol. 125, pp. 567-74.

Keblinski, P., Eastman, J.A. and Cahill, D.G. (2005), "Nanofluids for thermal transport", *Materials Today*, Vol. 8 No. 6, pp. 36-44.

Maïga, S.E.B., Nguyen, C.T., Galanis, N. and Roy, G. (2004), "Heat transfer behaviors of nanofluids in uniformly heated tube", *Superlattices and Microstructures*, Vol. 35 Nos. 3-6, pp. 543-57.

Corresponding author

N. Galanis can be contacted at: nicalas.galanis@usherbrook.ca